Research of Extension of the Life Cycle of Helicopter Rotor Blade in Hungary

M. Balaskó[1], G. Endrőczi[2], J. Veres[3], Gy. Molnár[3], F. Kőrösi[4]
[1]KFKI Atomic Energy Research Institute
H-1525 Budapest, P.O.Box 49. Hungary
[2]KFKI Research Institute for Particles and Nucleus
H-1525 Budapest, P.O.Box 49, Hungary
[3]Logistic Center of Hungarian Air Force
H-1885 Budapest, B.O.Box 25, Hungary
[4]Szent István University, Institute of Environmental
and Land Management, H-2100,
Hungary

Abstract

Combined measurements have been carried out at the Budapest research reactor, where the dimension of the radiography station was extended for the purpose the control the condition of helicopter rotor blades in the different period of their life time. High resolution radiography pictures were taken to find anomaly in the distribution of resin materials at the core-honeycomb-hull interfaces, failure at the "adhesive filling" and possible bondline flaws. Parallel to the radiographic visualisation vibration tests using the method of statistic energy analysis (focused on damping and energy distributions and propagation) served for control of dynamic behaviour of different aged structures. As a result of the work it is suggested that the combined application of the neutron-, X-ray radiography and vibration diagnostics might be a very useful method for the condition monitoring of helicopter rotor blades and other similar composite structures.

1. Introduction

The safe life testing of the rotary wing aircrafts, especially those of the rotor blades, is of paramount importance. The declaration of a structural failure that can grow to the point where structural integrity is affected comprises a central core. In this process the composition inspection, monitoring the rate growth of the defect in relation to the total flight hours are essential. The above demands underline the necessity in testing and applying new non-destructive testing (NDT) methods for inspection in service.

As a consequence, for the composite structure investigation of the rotor blades, three NDT methods: (i) Dynamic Neutron Radiography (DNR) (ii) Dynamic X-ray Radiography (DXR), and (iii) Vibration Diagnostics (VD) with Statistical Energy Analysis (SEA) were semi-simultaneously applied [1]. The used three NDT methods give complementary information upon the investigated object. The DNR is capable of investigating the irregularities in the fibre-glass/epoxy honeycomb structures. The details of metal parts and contactor of the heating elements are shown by DXR. The SEA and other VD methods are suitable for identifying small changes of structural damping. The experiments were performed at the Dynamic Radiography Station (DRS) of the Budapest (10 MW) research reactor where the necessary development, regarding the extension of the dimensions of the investigated object, was carried out. As a result the working place can inspect 10 m long and 0.7 m wide targets by neutron and X-ray radiography and by vibration diagnostics.

Paper presented at the RTO AVT Specialists' Meeting on "Life Management Techniques for Ageing Air Vehicles", held in Manchester, United Kingdom, 8-11 October 2001, and published in RTO-MP-079(II).

The main goal of the present study was to demonstrate the applicability of DRS in revelling the defects of the composite structures of helicopter rotor blades for Hungarian Air Force. In describing the defects the terms used by [2] for classifying the structural integrity and aging for helicopters were followed upon.

2. Methods

2.1. Radiography

Neutron radiography utilizes transmission of radiation to obtain information on the structure and/or inner processes of a given object. The basic principle of NR is very simple [3]. The object under examination is placed in the path of the incident radiation, and the transmitted radiation is detected by a two-dimensional imaging, as is illustrated in Figure 1. The NR

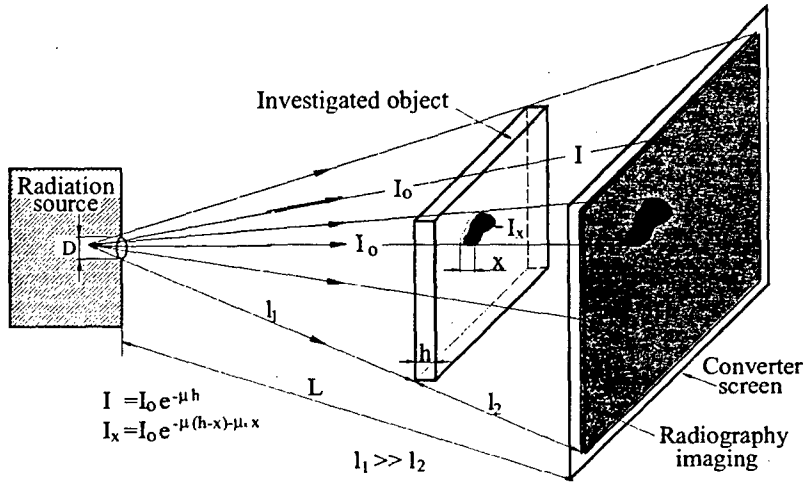

Fig. 1. General principle of radiography

arrangement consists of a neutron source, a pin-hole type collimator which forms the beam, and a detecting system which registers the transmitted image of the investigated object. The most important characteristic technical parameter of an NR facility is the collimation ratio *L/D* where *L* is the distance between the incident aperture of the collimator and the imagintg plane, *D* is the diameter of the aperture. This important parameter describes the beam collimation and will limit the obtainable spatial resolution by the inherent blurring independently from the properties of the imaging system. This unsharpness U_{beam} can be related to the distance between the object and the detector plane l_2 and to the *L/D* ratio

$$U_{beam} = \frac{l_s}{L/D}$$

Two opposing demands have to be taken into consideration when planning a radiography arrangement: if *L/D* is large then the neutron flux Φ_{NR} at the imaging plane is relatively weak but the geometrical sharpness is high, and vice versa.

$$\Phi_{NR} = \frac{\Phi_s}{16(L/D)^2}$$

where Φ_s is the incident neutron flux.

In radiography imaging the attenuation coefficient μ is a crucial parameter. The transmitted intensity of the radiation, I, passing through a sample with an average transmission of μ can be written as

$$I = I_o e^{-\mu h}$$

Where I_o is the incident intensity and h is the thickness of the sample. If there is any inclusion (inhomogeneity, inner structure) in the sample of thickness x and transmission μ_x then the transmitted intensity, I_x is given as

$$I_x = I_o e^{-\mu(h-x)-\mu_x x}$$

If the value of μ and μ_x are different from each other then the presence of the inclusion will provide a contrast in the radiography image.

The attenuation coefficient vs. atomic number is plotted in Figure 2 for neutron radiation and for gamma- and X-rays. Its value depends on both the coherent and incoherent scattering and on the absorption properties of the element(s). For neutrons μ, does not show any regularity as a function of atomic number, and for some of the lightest elements (H, B, Li) the attenuation coefficient is by two orders of magnitude greater than the corresponding parameter for most of the technically important elements, such as Al, Si, Mg, Fe, Cr. This fact is of practical importance, viz. neutrons penetrate almost all metals used for construction purposes with little loss in intensity; in contrast they are considerably attenuated in passing through materials containing hydrogen, such as water, oil or several types of synthetics. On the other hand in the case of X-ray and gamma radiation, this dependence may be characterized by more or less continuously increasing curves.. This means that the radiation is absorbed to a great extent by heavy elements whereas it penetrates light materials such as hydrogen without significant loss in intensity.

These differences for various radiations provide the possibility to gain complementary information by using all three types of radiation together.

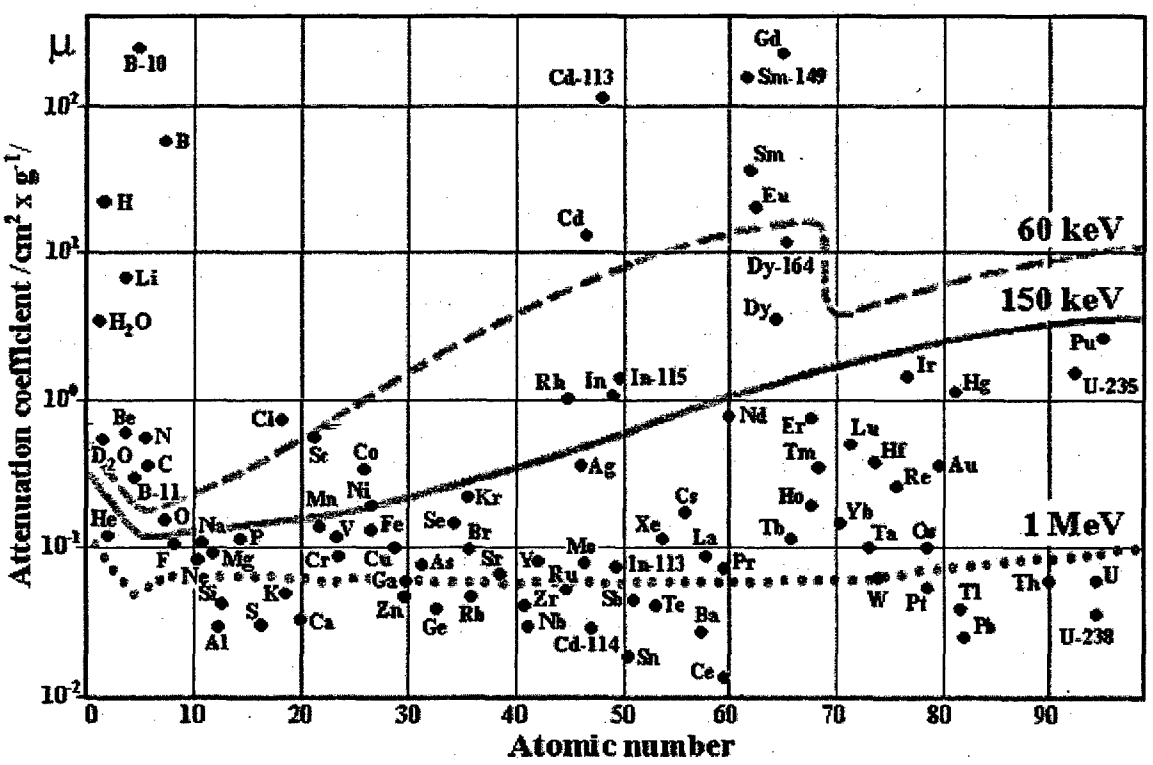

Fig. 2. Attenuation coefficient (note the logarithmic scale) of elements forneutrons (separate dots), for 1 MeV gamma-ray (dotted line), for 150 keV X-ray (solid line) and for 60 keV X-ray (dashed line)

2.1.1. Imaging techniques

In that neutrons are neutral particles a converter material - in NR generally a foil – is used to convert neutrons to another type of radiation, to enable them to be detected directly. Various detector systems are employed in NR: combinations of film and neutron sensitive converter foil, combinations of a light-emitting scintillator screen with a CCD camera and, more recently, imaging plates. Depending on the object to be investigated and the task to be solved, two basic types of NR are in use: static radiography and dynamic radiography (real-time). Both techniques provide averaged information on the investigated object in its depth. Neutron computer tomography (NCT) is a rapidly developing technique that provides information on the three-dimensional structure of a given object.

2.1.1.1. ***Static NR*** records a static picture of the object to be investigated. Even nowadays, film techniques are the most widely used. The information is not a priori obtained in digital form, but may be digitized with a scanner or densitometer. The most recent developments are the imaging plate (IP) system and the camera-based technique, both of which are now being used to a much greater extent.

The IP is a new film-like radiation image sensor based on photostimulated luminescence. It consists of a specifically designed composite structure that traps and stores the radiation energy. A polyester support film is uniformly coated with a photo-stimulatable luminescent material - barium fluorobromide containing a trace amount of Eu^{2+} as a luminescence centre ($BaFBr:Eu^{2+}$) – and it is then coated with a thin protective layer. The stored energy is stable until scanned with a laser beam whereupon the energy is released as luminescence. In the case of neutron sensitive IP the storage luminescent material is mixed with gadolinium oxide.

The camera-based system consists of a scintillator plate and either a low-light-level (LLL) video or CCD camera which records the light emitted by the scintillator. The images recorded by a CCD camera are inherently digital while those of a video camera can be recorded by video recorder or can optionally be digitized by a frame-graber. In static radiography the images recorded by the camera are integrated, and thus a static picture of good statistics may be obtained from the object.

2.1.1.2. Real-time NR is used to investigate movements inside the investigated object (flow of fluids in metal tubes, evaporation or condensation processes, two-phase systems). The imaging system consists of a scintillator plate that converts the neutrons into light which is detected by an LLL video camera with short imaging cycle or by a CCD camera. The individual images are registered and analysed on a time scale, they may be visualized on a monitor and recorded by a video recorder or by a computer. Compared with static NR this technique needs a relatively high neutron flux: at least 10^6 n cm^{-2} sec^{-1}.

2.2. Vibration Diagnostics (VD)

Parallel to the NDT measurements the Statistical Energy Analysis (SEA) as a vibration diagnostical tool were applied for the detection of structural behaviour of rotor blades.

The SEA applicable for structural identification where the modal density (amount of modes in a given frequency range) nearly constant.

The increasing development of SEA technique has been based on the early works of R.H.Lyon, P.W.Smith Jr. And G.Maidanik [4]. Prof. Lyon gave a complete summary of the theory and applications in 1975 and his work still serves as one of the most important refereences in the field.

In this theory the energy denotes the primary variable and displacement, velocity, acceleration, stress, etc. are deduced from that. The dynamical parameters of the system, the environment and responses are looked upon as statistical populations having known distributions. The structural identification is based on estimated dissipative properties using statistical variables [5].

The theory is based on the recognition that the kinetic and potential energies of similar natural modes or resonators whitin a frequency range are equal at resonacies. The energies of individual modes simply add to form the total system energy. The averaged displacements, velocities, accelerations, forces, mechanical impedances, energy losses or dampings, etc. are formulated in a system fashion to the description of a single mode resonator. Considering a group of resonators the basic expressions of responses and energies in the use of white noise excitation in a given frequency range can be formulated as follows:

$$< F^2 >_{\Delta f} = S_f \Delta f$$

$$< y^2 > = < \ddot{y}^2 > / \omega_0^2$$

where Δf - frequency band
f,ω - center frequency of a band
$<>$ - spatial average
S_f - power spectral density of force
F^2 - mean square value of force
y - displacement

This approximation is valid, when the resonant part dominates instead of mass.

The power input to the system, averaged over source location is:

$$P_{in} = S_f \Delta f \frac{\Pi n}{2M} = F^2 < G >$$

where n - modal density
G - conductance
M - mass

It can be seen that the modal density and the average conductance are closely related.

For a single resonator the loss factor is introduced as a phase angle of the complex Young's modulus

$$E = E_0(1 - i\eta),$$

for a viscous element

$$\eta = R / \omega M$$

The dissipation or damping properties of a system can be described using energy parameters. The measure of the dissipation of energy stored in the „loss-factor" which is the ratio of energy dissipated per unit time to average energy stored.

$$\eta = \frac{P_{diss}}{2 \Pi f E_{stored}}$$

The other important problem is the energy transfer between the structures. In the case of multimodal resonator systems vibration energy is transferred from one subsystem to the other

by similar modes. The transferred energy is respect to the stored energies and the involved modes. For arbitrary two systems, it was found to be,

$$P_{i,j} = \omega\eta_{i,j}E_{i,total} - \omega\eta_{j,i}E_{j,total}$$

According to these equations, the SEA calculates the flow and storage of vibration energies in a complete system, identifies the structure as a series of energy storage and dissipating elements. Thus in a general SEA model the structures are idealized into an assemblage of individual subsystems having similar and significant energy storage modes.

In the model the input powers, $P_{i,in}$, resulted from acoustical noise or mechanical excitation, have not sensitivies to the state of coupling between subsystems. The dissipated powers, $P_{i,diss}$, represent the energy lost to mechanical vibration and depends only on the amount of energy stored in the subsystem. The transmitted power, Pi,j , represents the energy exchanged between subsystems. The dissipated power cannot be returned to the system. The amount of energy stored in the subsystem is determined by available modes N1...Nn within the frequency band. The following basic relationships concern the model without detailed verifications:

The power flow between subsystems is

- proportional to the actual vibration energies of subsystems
- directly proportional to the difference in decoupled energy of subsystems
- the average power flow is from the subsystem of greater to lesser energy
- equal difference of subsystem energies is either direction will result in an equal power flow (the power is reciprocal)

For the i'th subsystem the power balance is:

$$P_{i,in} = P_{i,diss} + \sum_{j=1}^{N_i} P_{i,j} \qquad i \neq j$$

The relations between power, stored energy and loss-factors can be written in matrix wherein the structure is identified by the loss factor matrix. The loss factor matrix, the vector of energy stored and the input powers stand for the stiffness matrix and vectors of displacements and applied forces.

$$\underline{\underline{\eta E}} = \underline{P_{in}} / \omega$$

$$\underline{\underline{J}}\,\underline{y} = \underline{F}$$

3. Experimental facility

Measurements were performed at the Dynamic Radiography Station (DRS) at the 10 MW Research Reactors in Budapest. The Figure 3 shows the arrangement of the DRS. Its main parameter are the follows: 10^8n.cm^{-2}.sec^{-1}, the collimation ratio (L/D): 170, the diameter of the beam: 180 mm. The X-ray generator was adjusted to 150 kV and 3 mA. The information carrying radiography images were converted into light ones by NE426 scintillator screen for neutron radiography and NaCs single crystal was used for X-ray radiography. The obtained light images were detected 10^{-4} lux low light level TV camera (ITV1122 type) and registered by S-VHS videocassette recorder [6]. For digitalization and image processing QUANTEL SAPPHYRE V.05 and IMAN a β version softwares were applied.

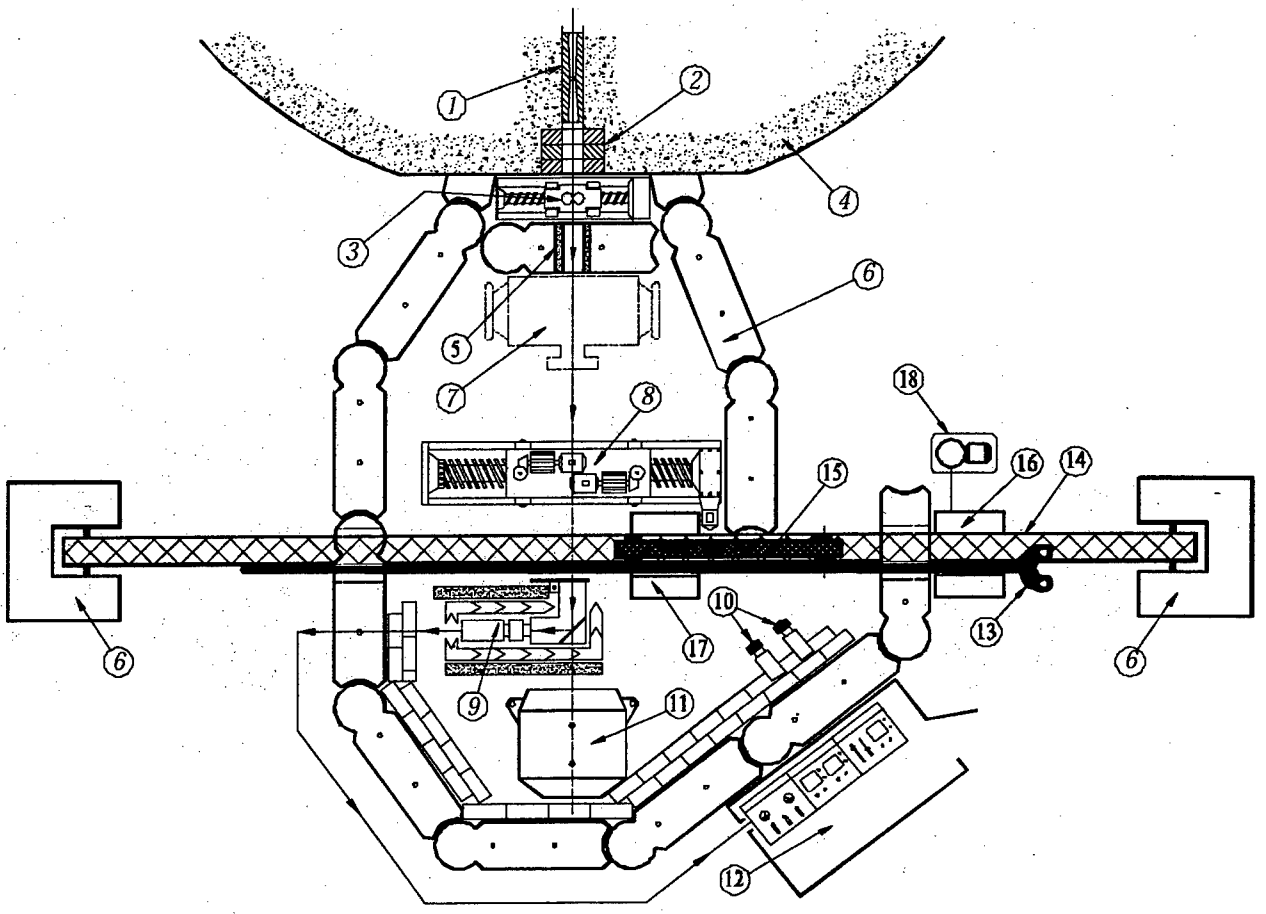

1. Inside collimator
2. Iron shutter system
3. Beam diameter changer and filter unit
4. Reactor shielding
5. Outside collimator
6. Biological shielding
7. X-ray generator
8. Investigated object with remote control mechanism
9. Imaging system with low light level TV camera
10. Background TV cameras
11. Beam stop
12. Control cabin
13. Rotor blade (~ 10 m)
14. Rail of the rotor blade transporter
15. Transporter of the rotor blade
16. Moistening module
17. Drying unit
18. High pressure water pump

Fig. 3. Schematic arrangement of Dynamic Radiography Station at the Budapest research reactor

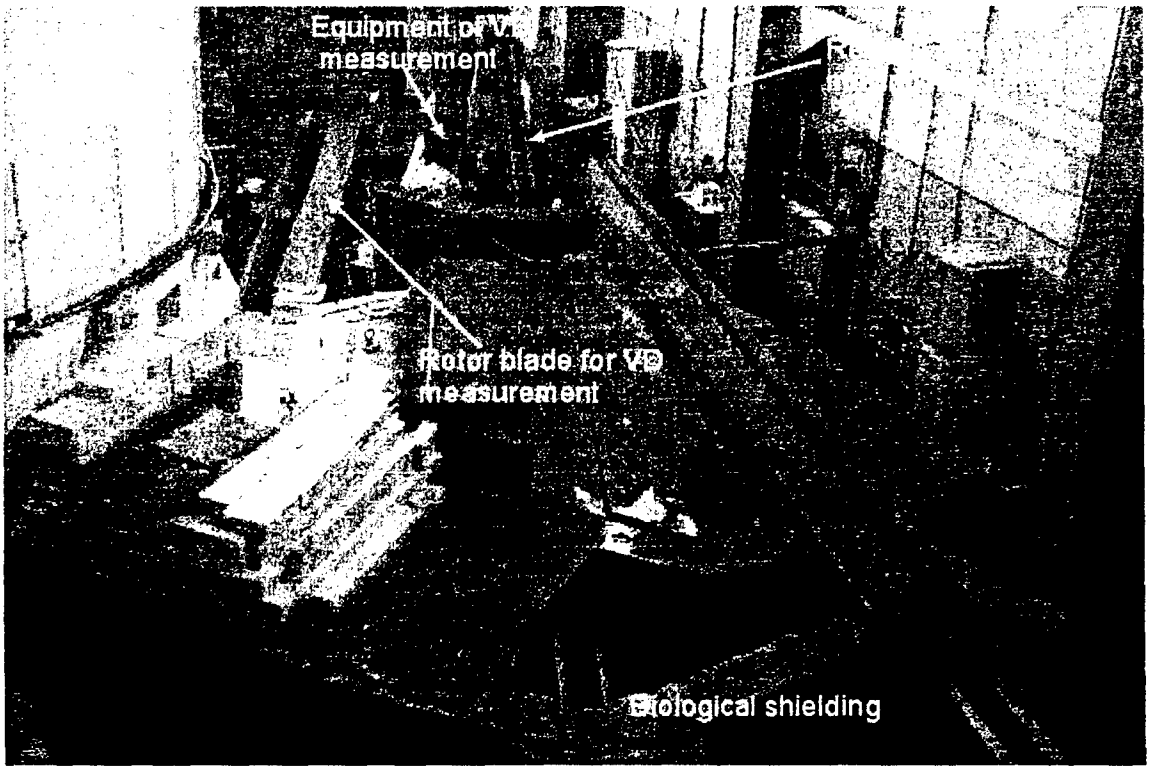

Fig. 4. Overview of the Dynamic Radiography experimental station

We could verify the state of rotor blades in dry and wet conditions simulating the complicated weather circumstances. The moisture was served by the Moistening module and the necessary water was supplied by the closed-circulated High pressure water pump. The overview of the experimental setup is shown in Figure 4. As it can be observed in the Figure 4, the complete rotor blade can be placed and moved in the neutron and X-ray beam. Simultaneously with the radiography visualization, on the other blade the vibration sensors were placed at given points of the blades and the damping characteristics were investigated. The registered vibration noises were analysed with a dual-channel real time frequency analyser (BK2035). In addition to the Statistical Energy Analysis measurement a small exciter table (BK4810) and an impedance head (BK 8000) used.

4. Investigated object

The lifetime extension of the rotary wings is a main achievable goal for the helicopter serving in the Hungarian Army. Majority of the helicopters, Mi 8 and Mi 24 types in the Hungarian Army's inventory are several decades old and required to continue their service even longer. One of the most important parts of them is the rotor blade. They are made of composite structures and contain 21 pieces of honeycomb construction with many bonded surfaces. The 21 sections of the rotor blades were divided into 4 zones horizontally and 53 fields in

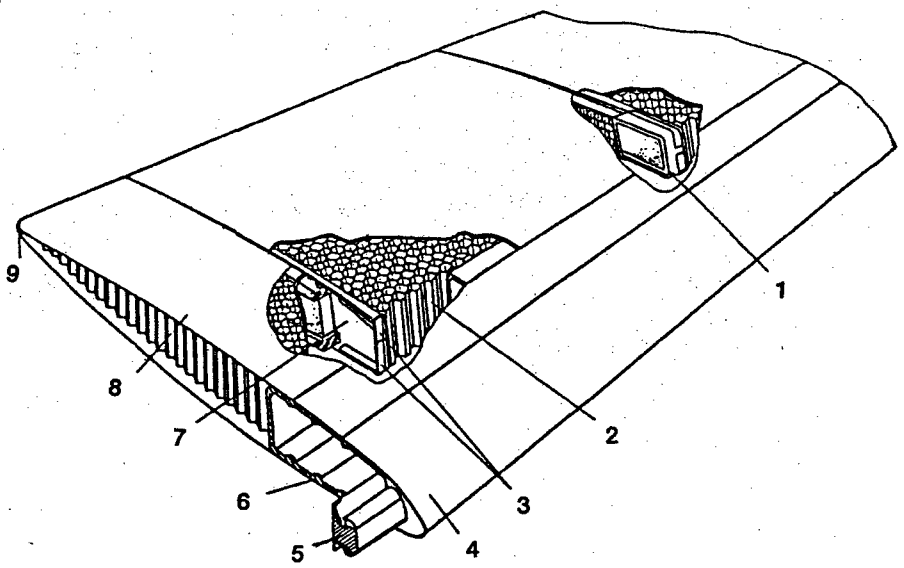

1. **balance seal**
2. **honeycomb structure**
3. **face-rib**
4. **anti-ice heater**
5. **anti-flatter weight**
6. **spar**
7. **rib.**
8. **skin**
9. **backside stringer**

Fig. 5. The inner structure of the rotor blade

vertically. The key part of the rotor blade comprises the aluminium alloy metal main holder bonded to the honeycomb structure as seen in Figure 5.

5. Measurement

The description of the measurement was very prudent regarding the dangerous nature of the radiation material testings both neutron an X-ray. On schedule of the inspection the first step was the VD measurement, the second step was an NR inspection in dry condition, the third step was the NR inspection in wept condition, the fourth step was the XR test and the last one was another. VD measurement again. A new (RLU) and (RL-10) rotor blades were verified by this inspection technology. We are able to declare that we did not experience any effect of the radiation techniques.

5.1. Neutron radiography

The NR is capable of detecting and visualizing irregularity and defects in composite construction. One of the main advantages of the NR constitutes that it is especially sensitive in revealing the hydrogen- (water) content and its distribution in the investigated object. To this end a special analysis was designed and carried out at DRS. In the first step the all surface of the blade was scanned with DNR in dry conditions. In the second step having the rotor blade being moistened, the scanning operation was repeated to follow the penetration sites and distribution of water in the composites structures.

The most important bond is the one that sticks together the aluminium alloy metal main holder and the honeycomb structure.

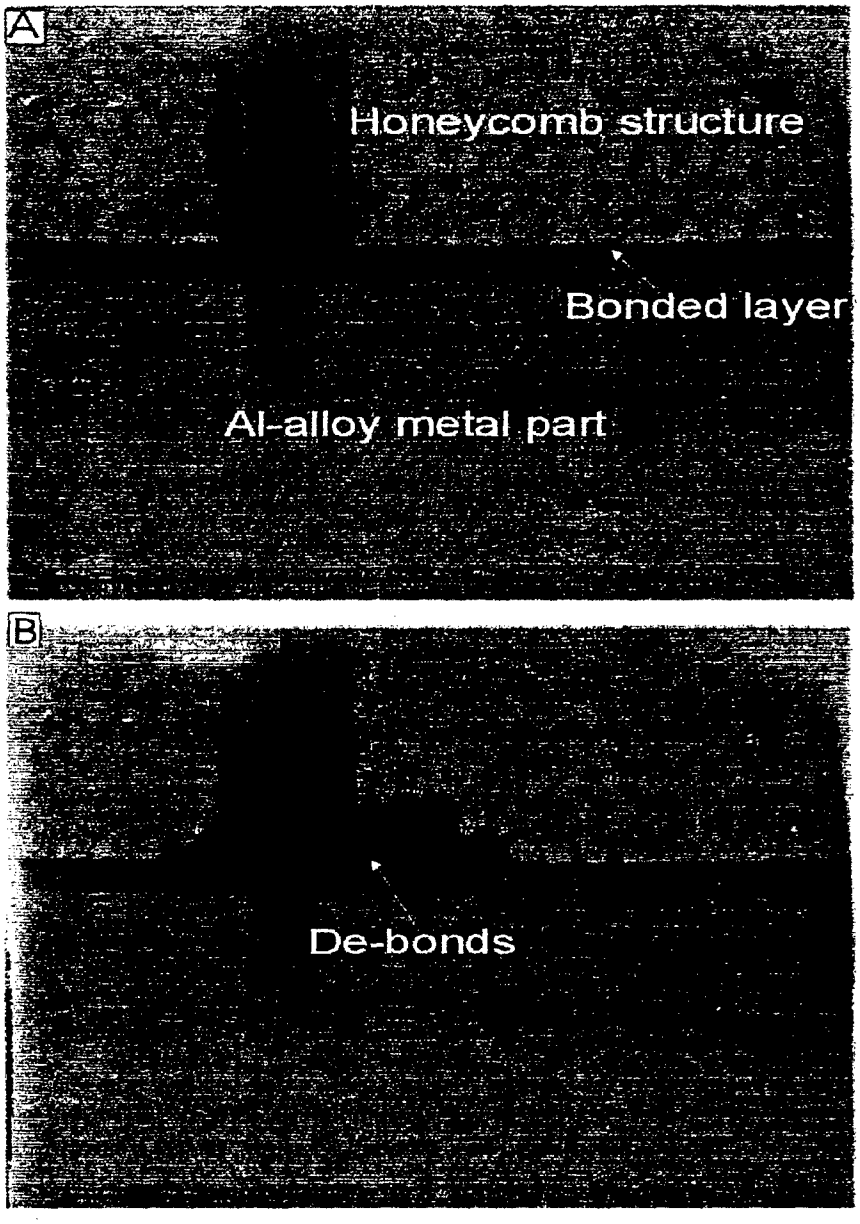

Fig. 6. DNR images of the de-bonds. "A" scanned without water "B" contrasted by water

Fig. 6/a shows this part between the 13th and 14th section. The bonded area is seen as a horizontal black line under dry condition. In the Fig. 6/b the efficacy of moistening in unveiling the damage of the gum sealing at the border of the sections by centrifugal force was explicitly demonstrated.

The other failure makes up the delamination within piles of a laminate as displayed in Fig. 7. This failure was recognized at the 4th band, 49th field of RL 10 rotor blade (Fig. 7A), with the most affected areas being displayed with curves. The Figure 7B shows Sobel-enhanced edges of the delamination, while the Fig. 7C illustrates the Fig. 7D representation of the concerned area. This type of failure may be brought about by improper surface preparation, contamination and embedded foreign matter.

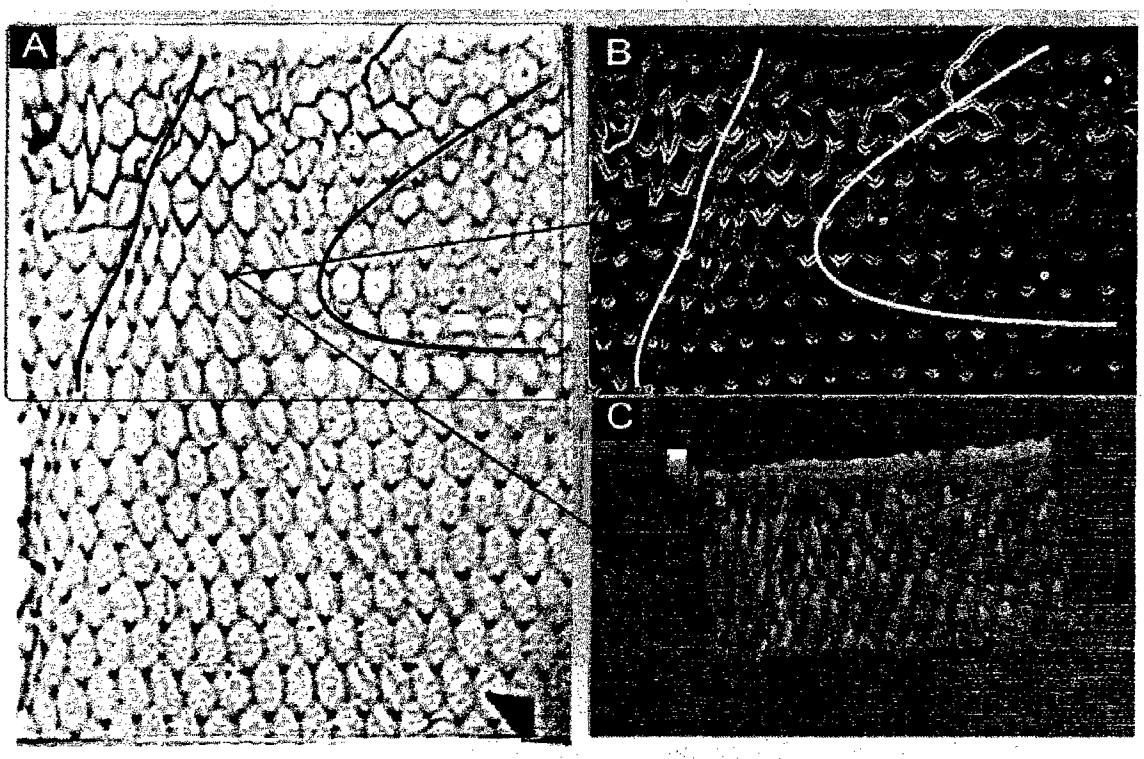

Fig. 7. Represetation of fiber misalignment. "A" shows the DNR image; "B" stands for the processed image of the marked area; "C" illustrates the 3D plot of the images. The curves demonstrate the affected area

The DNR image exhibited in Fig. 8 discloses another type of defect, i.e. resin-rich areas and resin-starved ones. Resin rich areas are localized, and filled with resin or lacking in fiber. The defects is caused by improper compaction or bleeding. Resin-starved areas are localized with insufficient resin evident as dry spots or areas. (These defect were located on the RL-10 blade: 4^{th} band 35-36^{th} field, 8^{th} section.)

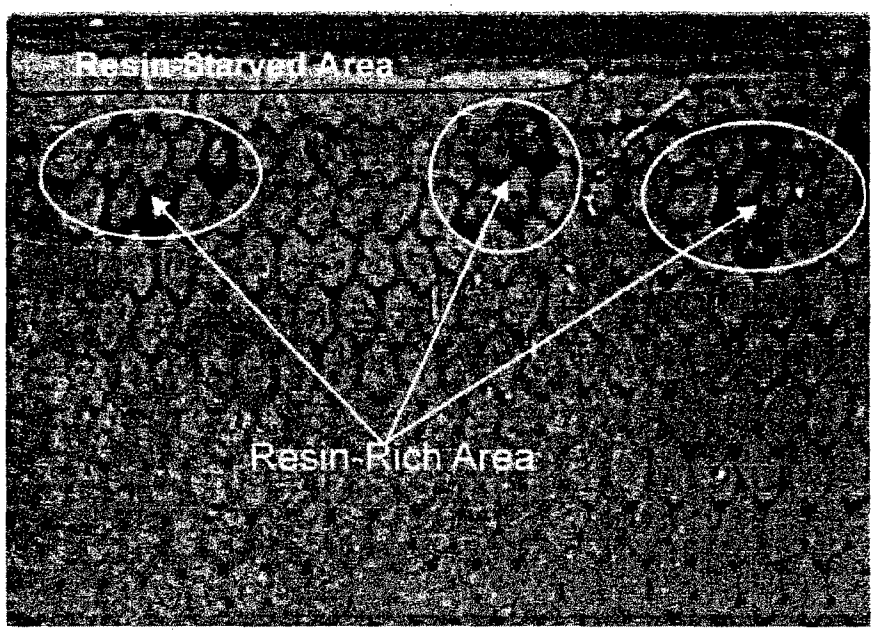

Fig. 8. Resin-rich and resin-starved areas as revealed by DNR imaging

Fig. 9 reveals honeycomb misalignment ('A'), porosity ('B'), and damage of the gum sealing ('C'). Honeycomb misalignment is distortion of the piles resulting in changes from the desired orientation. These defects are due to improper lay-up and cure. Porosity ('B') is pockets within the bonding material. They are begot by entrapped air and gas bubbles, and caused by volatile substances, improper flow of resin and unequal pressure distribution. De-bonds ('C') were discussed above. (These defects were identified on RL-10 blade: 3rd . band 37th field, 16th section amid moistened condition.

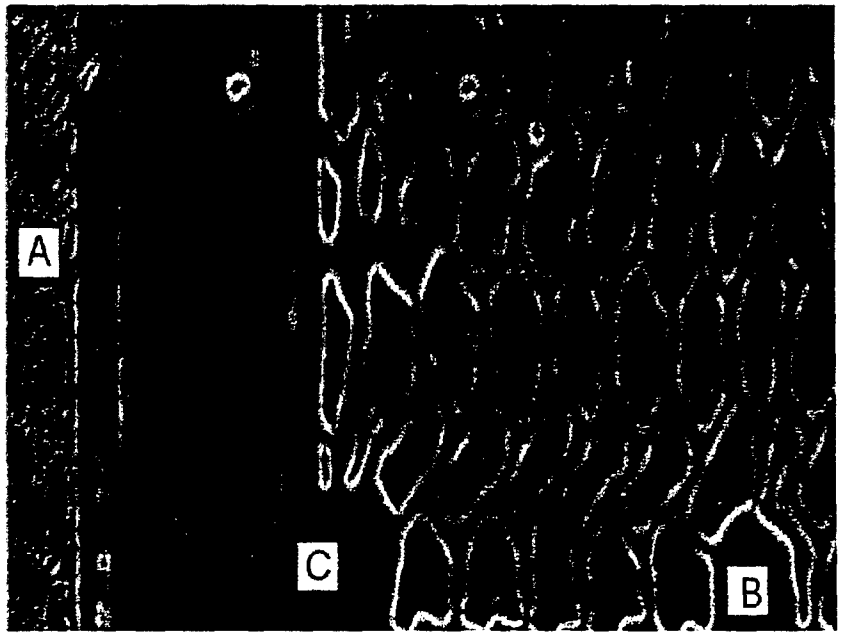

Fig. 9. Analyzed DNR image, demonstrating various defects: "A" honeycomb misalignment; "B" porosity; "C" damage of the gum sealing

5.2. X-ray Radiography

X-ray radiography is a complementary and useful tool in detecting the structural integrity of metal parts of the blades. Fig. 10 shows the heating element arrangements and their contacts on the blade. The measurement was performed on RL-10 rotor blade, iv.Band 54.field, 1st section.

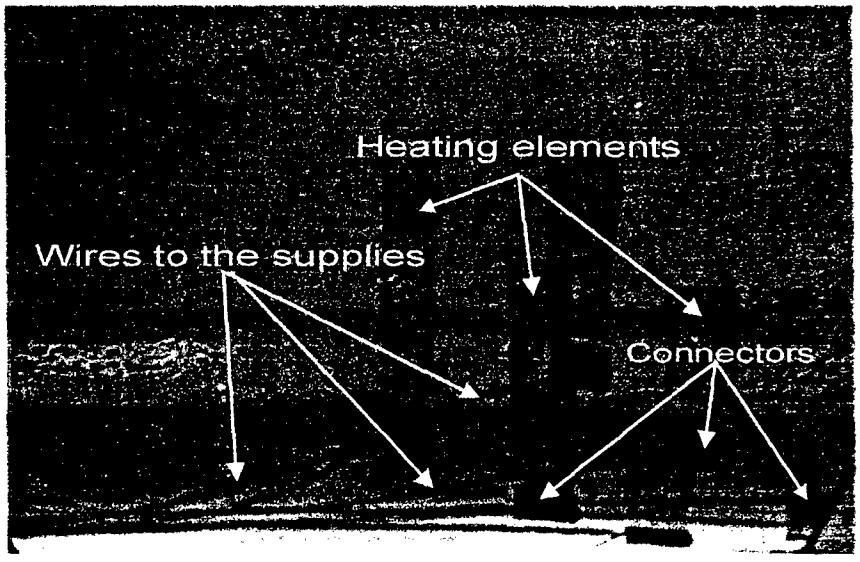

Fig. 10. Metal parts of the rotor blade visualized by XDR

5.3. Vibration Diagnostic

After the first laboratory tests series of different aged blades were measured. A simple two subsystems SEA model was used for the structural identification of rotor blades. During the measurements the sensors were placed at the 2., 5., 8., 14., 17., and 19. sectors at the border line of core and honeycomb section, at the 11. sector an exciter table with impedance head served for power input. The stored vibration energy, loss factors (proportional to damping) and their ratios were calculated in different frequency ranges. The quantity indicated on Fig 11. represent the general condition of blades.

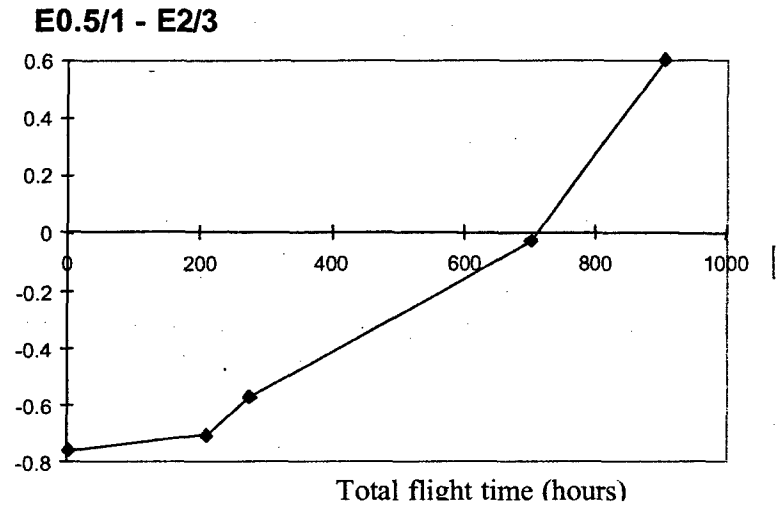

Fig. 11. Difference of stored energy between frequency bands at given flight times

Another parameter in the Fig. 12. demonstrates that distinct differences in the vibration energy collector capacity between new and old rotor blades in dry and moistened conditions. At a frequency band of 2.5-3 kHz exciting energy, the energy storage for the either the new or the old one displayed two peaks. The damping capacity for the new one was considerably lower than that for the old one. While the moistened blade exhibited no peak vs. the sensors positions. Another important observation from the SEA model that with increasing the frequency of exciting energy the energy storage capacity of the new blade's the first position, i.e. the blade end, was considerably, about 2 order, higher. It underlines the significantly less damping property of that section of the new rotor blade, as it is shown in the Fig. 13.

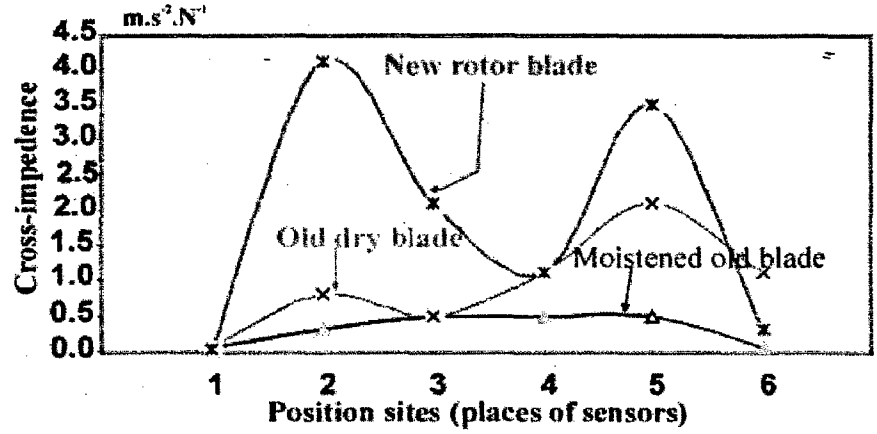

Fig. 12. The stored vibration energy of the old and new rotor blades at a frequency band of 2.5-3kHz

These evidences clearly prove that applying the two subsystems SEA models into the blade adequately indicate the differences in the conditions of the blades. According to the SEA measurement no damage to the blade was caused either by neutron or X-ray radiation during the test.

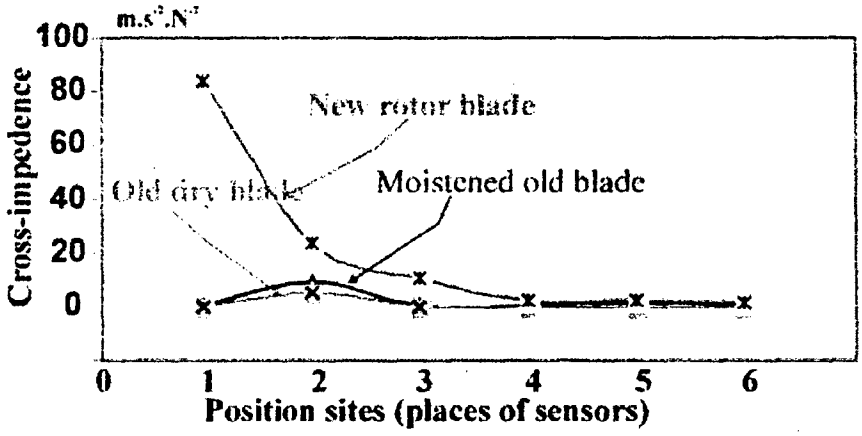

Fig. 13. The stored vibration energy of the old and new rotor blades at a frequency band of 6-8 kHz

6. Conclusions

The joint application of dynamic neutron and X-ray radiography and the statistical energy analysis proved to be applicable in the visualizing and detecting changes in the inner details of multiplayer-honeycomb structure of the helicopter rotor blades.

The defects revalued by DNR were:

- Delamination
- Porosity
- Resin-rich areas
- Resin-starved areas
- Honeycomb misalignment
- Damage of the sealing
- De-bonds.

By using DXR the metal functioning part of the rotor blade can be inspected.

The SEA technique adequately and supplementary to the DNR and XNR characterized the stochastic amounts of micro-cracks of the rotor blades in connection with flight hours.

References

1. M. Balaskó, G. *Endrõczi, J.* Járfás, Gy. Makai, Study of complex composite-metal structure with dynamic neutron radiography and vibration diagnostics. Proc. 7th European Conference on Non-destructive Testing (ECNDT'98) Ed. B. Larsen. Copenhagen, (1998). Pp.341-348.

2. J.K. Sen and R.A. Everett, Structural integrity and aging related issuez for Helicopters, RTO/NATO 2000, ISBN92-837-1051-7, pp.5.1-5.21.
3. M.Balaskó, E.Sváb, Neutron radiography in research and development, Nukleonika 39, 1-2(1994) pp.3-22.
4. R.H. Lyon, Statistical Energy Analysis of Dynamical System, MIT Press 1975.
5. B.L. Clarkson et al, Experimental Work to Evaluate Parameters Required in the SEA Prediction Method, ESA Contract report on 4100/79/NL/PP. Rider1, 1981
6. M.Balaskó, E.Sváb, Dynamic neutron radiography instrumentation and applications in Cental Europe, Nuclear Instruments and Methods in Physics Research A377(1996)pp.140-143.